Hyperfine Interactions 123/124 (1999) 721–739

Time-delayed interferometry with nuclear resonant scattering

Yuji Hasegawa and Seishi Kikuta

Department of Applied Physics, The University of Tokyo, Hongo, Bunkyo-ku, Tokyo 113, Japan

Experimental results of "time-delayed interferometry" with nuclear resonances at KEK are reported. Mössbauer nuclei were used as a cavity for X-rays in these experiments. Various interference effects were observed on a macroscopic scale with the "perfect crystal" interferometer. The property of coherence and the combined system showed some characteristics of collective nuclear excitations, e.g., absorption of photons without the reduction of the detection probability, the phase information transfer, and spontaneous emission with phase relation. Interferometry with a large optical path length, i.e., 4.2 mm, was accomplished with a wave-front division type X-ray interferometer. An interference experiment with a vibrating resonant scatterer exhibited quantum beat oscillations in the time domain. Interferograms with samples of different thicknesses revealed a remarkable phase shift of π in the time evolution, which is induced by the dispersion effect at the nuclear resonance. A future perspective of time-delayed interferometry is also presented, e.g., for temporal phenomena in nuclear resonant scattering. Time-delayed interferometry has established a new field of X-ray optics, which can be of help for fundamental, nuclear, and solid state physics.

1. Introduction

Interferometry with wavelengths on the Angstrom scale has developed quite steadily. The first experimental accomplishment was reported in 1965 by Bonse and Hart [1,2]. Successive Laue diffractions were used for the beam handling, i.e., splitting, reflecting and recombining. This type of interferometer is called the triple-Laue (LLL) interferometer. Other types of interferometer were investigated, e.g., triple-Bragg (BBB) [3], double-Laue (LL) [4] and double-Bragg (BB) [5]. Among them the LLL-interferometer has been used most. The LLL-interferometer has components equivalent to the Mach–Zehnder interferometer in the visible-light region.

The advent of the X-ray interferometer stimulated new investigations in the field of fundamental and applied physics. For instance, the extremely high sensitivity of the interferometer made it possible to measure the lattice parameter with high precision [6]. Precise measurements of the anomalous dispersion were achieved with the use of synchrotron radiation (SR) [7] or a multiple-wavelength technique [8]. Together with the recent development of SR the X-ray interferometry has been applied to experiments of optical interest in the X-ray regime, e.g., to a general mixture of interfering

beams [9] or to the statistical fluctuation of the elementary component in a strong gas absorber [10].

The time-delayed scattering via the 14.4 keV Mössbauer resonance of ^{57}Fe has been studied for more than a decade, using a pulsed SR source in combination with a delayed coincidence technique [11]. This process has a close analogy to the free-induction decay in other regimes of the electromagnetic spectrum, which was extensively investigated particularly in other optical [12] and radio-frequency (RF) [13] regimes. In 1991 delayed coherent nuclear forward scattering of SR by a polycrystalline Fe foil was measured [14]. This opened up further possibilities to apply nuclear resonances in interferometry, since forward scattering does not change beam paths.

The nuclear resonant scattering exhibits intensity modulations in subsequent decays due to the coherently excited energy levels of nuclei split by hyperfine interaction. Similar quantum beats were reported with the use of Ba atom excitations in the visible-light region [15]. They emphasized that "in such 'single atom' quantum beats, the interference occurs between decay channels of single atoms, and not as interference between emission of different atoms". It is worth noting here that this argument can not be applied to the Mössbauer nuclear excitations by SR, where interference between beams emitted by different nuclei is observed.

2. Coherent property of nuclear resonant scattering

Coherence appears in many aspects of nuclear resonant scattering. What kind of effects are observed when both split beams experience nuclear resonant scattering? Here a direct observation is described of the interference between the resonantly scattered beams, which are emitted by different nuclei by nuclear resonant scattering [16]. High visibility interference oscillations were obtained, showing the coherent nature of two split beams after the nuclear resonant scattering. This result comes from the fact that these beams are superposed and coincide completely in the time domain after nuclear resonant scattering.

A measured time-spectrum of nuclear resonant forward scattering with the use of an ^{57}Fe foil, about 4 μm thick, is shown in figure 1. A fast detector with TAC enables us to pick up the delayed nuclear resonant scattering events of this time-spectrum. A schematic view of the experimental setup is shown in figure 2. The incident beam was monochromatized to 8 meV through two Si(10 6 4) asymmetrically and symmetrically channel-cut monochromators in a dispersive arrangement placed downstream of the Si(1 1 1) double crystal pre-monochromator. An LLL-interferometer made from a Si single crystal was adjusted to give (2 2 0) reflections. The cross section of the incident beam was reduced to 5.0×0.2 mm^2. Fe foils enriched in ^{57}Fe of about 4 μm thickness were inserted between the first and the second plate of the interferometer as nuclear resonant scatterer. A parallel-sided Si wafer of 290 μm thickness was inserted between the second and the third plate of the interferometer as a phase shifter. A variation of the phase shift was obtained by rotating the wafer. A fast

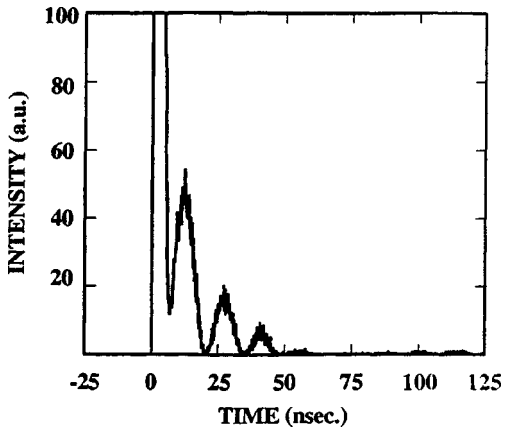

Figure 1. A measured time spectrum of nuclear resonant forward scattering with the use of an ^{57}Fe-foil about 4 μm thick. The effect with a delay of some tenths ns is shown.

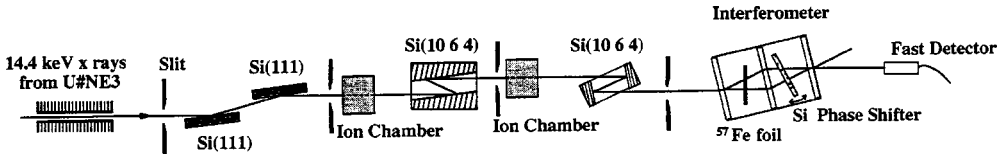

Figure 2. Schematic view of the interference experiments. The incident beam is monochromatized to $\Delta E = 8$ meV and its energy can be adjusted at and off resonance. In the triple-Laue interferometer, the phase shifter, made from a Si wafer, and the nuclear resonant scatterer, an ^{57}Fe foil, are inserted [16].

detector was put in the interfering O-beam, i.e., the interfering beam in the forward direction.

The delayed gate opening time for measuring the interference oscillations was set between 37 and 89 ns, so that only the resonantly scattered yields were counted without the prompt component. Interference oscillations were measured by shifting the relative phase. The data with least squares fits are shown in figure 3. An almost complete interference oscillation above the background is seen for counts at resonance. In contrast, only the fluctuation of the background is seen for counts off resonance, which was collected by tuning the monochromator 156 meV from the resonant energy.

The observed interference oscillations arise from the interference between two split beams, into both of which the ^{57}Fe foil was inserted. Since the gate (37–89 ns) was used in the counting system, only photons emitted through resonant scattering are responsible for these oscillations. It should be mentioned here that the time-delayed scattering for two split beams occurred at a macroscopic distance and with a time interval larger than the coherence time of the incident beam. In the X-ray experiments, the photon numbers are quite low and self-interference of single photons is observed. The present results indicate that

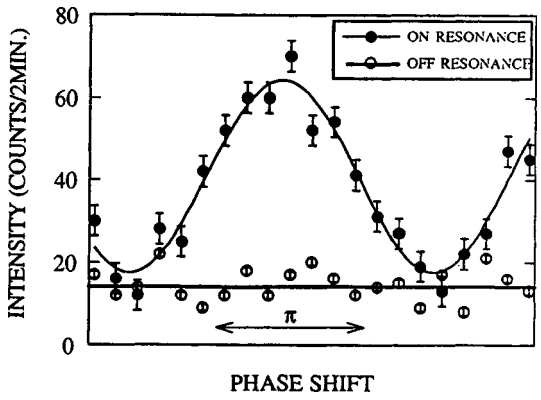

Figure 3. Interference oscillations with least squares fits for energies at and off resonance. A high visibility interference oscillation is observed at resonance, while only the background fluctuation is observed off resonance [16].

(i) two split beams after nuclear resonant scattering are coherent, and

(ii) even an incident beam with a single photon is split into two paths and creates nuclear resonant scattering in both paths.

Moreover, the visibility of the interference oscillations with delayed gate was as high as that without gate. This demands that the delayed-scattered wave fields in both beam paths are completely coincident in the time domain. In other words, they get exactly the same delay by nuclear resonant scattering.

In the X-ray experiment contributions from other than the single photon state are negligibly small, even if highly brilliant SR is utilized. Thus, by using N-representations the components of more than two occupied states are negligible. For simplicity, picking up the main contribution of the single photon state $|1\rangle$, the state of the incident beam $|\Psi_{\rm inc}(t)\rangle$ is given by

$$\big|\Psi_{\rm inc}(t)\big\rangle = \alpha|1_{\mathbf{k}_0}\rangle, \tag{2.1}$$

where $\mathbf{k}_0$ represents the wave vector of the incident beam and α the coefficient.

The combined state of the beam as well as the nuclei after scattering $|\Psi_{\rm sc}(t)\rangle$ is given by

$$\begin{aligned}\big|\Psi_{\rm sc}(t)\big\rangle = \alpha\Big\{ &\sum_j \sum_{\mathbf{k}} \exp(-\mathrm{i}\mathbf{k}_0\cdot\mathbf{r}_j) \\ &\times \big[\exp(\mathrm{i}\mathbf{k}\cdot\mathbf{r}_j)\beta^j_{\mathbf{k}}(t)\big|\{g_i\};1_{\mathbf{k}}\big\rangle + \gamma^j(t)\big|\{g_{i\neq j}\},\mathrm{e}_j;0_{\mathbf{k}_0}\big\rangle\big]\Big\},\end{aligned} \tag{2.2}$$

where j, $\mathbf{k}$, $\mathbf{r}$, β, and γ represent the jth nucleus, the wave vector of the emitted beam, the positions of the nuclei, and the coefficients of the corresponding states, respectively. $|\{g_i\};1_{\mathbf{k}}\rangle$, and $|\{g_{i\neq j}\},\mathrm{e}_j;0_{\mathbf{k}_0}\rangle$ represent the states in which all nuclei are in the ground state with emitted photon of wave vector $\mathbf{k}$ and the jth nucleus which

is excited after absorbing the photon with wave vector $\mathbf{k}_0$. Here, since the forward scattering is dominant for polycrystalline foils, the state $|\Psi_{\rm sc}(t)\rangle$ reduces to

$$\big|\Psi'_{\rm sc}(t)\big\rangle = \alpha\Big\{ \sum_j \big[\beta^j(t)\big|\{g_i\}; 1_{\mathbf{k}_0}\big\rangle + \exp(-\mathrm{i}\mathbf{k}_0\cdot\mathbf{r}_j)\gamma^j(t)\big|\{g_{i\neq j}\}, \mathrm{e}_j; 0_{\mathbf{k}_0}\big\rangle\big]\Big\}. \quad (2.3)$$

For simplicity, $\beta^j_{\mathbf{k}_0}(t)$ is written as $\beta^j(t)$.

With the help of eq. (2.3), after going through the interferometer, the state $|\Psi(t)\rangle_{\rm int}$ is written in the form

$$\begin{aligned}\big|\Psi_{\rm int}(t)\big\rangle &= \frac{\alpha}{2}\Big\{ \sum_{j_{\rm I}} \big[\beta^{j_{\rm I}}(t)\big|\{g_i\}; 1_{\mathbf{k}_0}\big\rangle + \exp(-\mathrm{i}\mathbf{k}_0\cdot\mathbf{r}_{j_{\rm I}})\gamma^{j_{\rm I}}(t)\big|\{g_{i\neq j_{\rm I}}\}, \mathrm{e}_{j_{\rm I}}; 0_{\mathbf{k}_0}\big\rangle\big]\Big\} \\ &\quad + \frac{\alpha}{2}\mathrm{e}^{\mathrm{i}\phi}\Big\{ \sum_{j_{\rm II}} \big[\beta^{j_{\rm II}}(t)\big|\{g_i\}; 1_{\mathbf{k}_0}\big\rangle + \exp(-\mathrm{i}\mathbf{k}_0\cdot\mathbf{r}_{j_{\rm II}})\gamma^{j_{\rm II}}(t)\big|\{g_{i\neq j_{\rm II}}\}, \mathrm{e}_{j_{\rm II}}; 0_{\mathbf{k}_0}\big\rangle\big]\Big\},\end{aligned} \quad (2.4)$$

where ϕ represents the phase shift due to the phase shifter, and the subscripts I and II denote the split beam path I and path II in the interferometer, respectively. Complete coincidence in the time domain demands

$$\sum_{j_{\rm I}} \beta^{j_{\rm I}}(t) \;=\; \sum_{j_{\rm II}} \beta^{j_{\rm II}}(t),$$

so one sets here

$$\beta(t) \equiv \sum_{j_{\rm I}} \beta^{j_{\rm I}}(t) = \sum_{j_{\rm II}} \beta^{j_{\rm II}}(t).$$

The measured intensity $I_{\rm int}$ is given by

$$I_{\rm int} = \int_{t_1}^{t_2} \big\langle \Psi_{\rm int}(t)\big|\big\{a^\dagger_{\mathbf{k}_0}\cdot a_{\mathbf{k}_0}\big\}\big|\Psi_{\rm int}(t)\big\rangle\,\mathrm{d}t \quad (2.5)$$

$$= \int_{t_1}^{t_2} \frac{|\alpha|^2}{2}\big|\beta(t)\big|^2\,\mathrm{d}t\cdot(1-\cos\phi), \quad (2.6)$$

where $a^\dagger_{\mathbf{k}_0}$ and $a_{\mathbf{k}_0}$ are the creation and annihilation operators. In the experiments, t_1 and t_2 were set to 37 and 89 ns, respectively, and a clear interference oscillation due to ϕ was observed.

It must be emphasized that the interference demands coherent superposition of the beams emitted in each path by nuclear resonant scattering. Thus, the observed interference arises from beams emitted by different nuclei. It is reasonable to assume that not a single nucleus but an ensemble of many nuclei undergoes nuclear resonant scattering in each of the two paths. In time-delayed interferometry one can see the superposition of excited and ground states of nuclei as well as the superposition of

the beams of path I and path II. The former superposition is related to a continuous emission. One of the interpretations of the intermediate state of the continuous emission is the coexistence of the emitted photon and the emitting nuclei.

From a study of the emission and the absorption of the radiation field, i.e., the photoelectric effect, it is concluded that an "electromagnetic wave can change its energy only in units $h\nu$ [17]". In addition, anti-coincident detection is observed in a single-photon beam splitting experiment, which shows that the detection in one path will reduce the probability of detecting the photons in the other paths. The above interferometry, however, shows that even an incident beam with a single photon can bring forth the nuclear resonant scattering in both paths and those two beams, which are emitted through the resonant scattering, are superposed and interfere. The nuclear resonant scattering in one of the paths cannot reduce the probability of detecting the photons in the other paths. This suggests that the absorption of photons need not be accompanied by the reduction. These nuclear resonances should be regarded as a "scattering", after which all the beams – transmitted and scattered in any direction – are superposed. The former can preserve the nonreduction. The noteworthy difference from the conventional scattering by electrons is that the absorbed photons can be thought of as emitted not instantaneously but continuously.

3. Phase transfer in nuclear resonant scattering

Nuclear resonant scattering demands the consideration of the combined state of the radiation field and the nucleus. Combined systems are known in other regimes, e.g., combination of two particles [18,19] as well as that of the radiation field and an atom in a cavity [20]. They show a notable correlation and/or interference of the probability amplitudes of the combined states. Here the dependence of the interference pattern on the phase shift *before* nuclear resonant scattering is demonstrated [21]. The observed interference pattern implies that the intrinsic phase information is transferred to the re-emitted beam through the absorption and the delayed re-emission in the resonance. Since the essential contribution of the incident photon state to the experimental results is the single photon state, the photon state after absorption that has excited the nuclei may be regarded as the vacuum state. The possibility of storing the intrinsic phase information in the vacuum state of the quantized radiation field is shown combined with the state of the nucleus at the nuclear resonance.

A schematic view of the experimental setup is shown in figure 4. The delayed coincidence system as well as the monochromators were essentially the same as those in earlier work [16]. The experiment was performed to demonstrate the interference occurring due to a phase shift introduced before nuclear resonant scattering with its time-delay took place. Thus, while a phase shifter was inserted between the first and the second plate of the interferometer, a nuclear resonant scatterer was inserted between the second and the third plate. As a phase shifter a parallel sided Si wafer of 290 μm thickness was used and a variable phase shift was introduced by rotating this

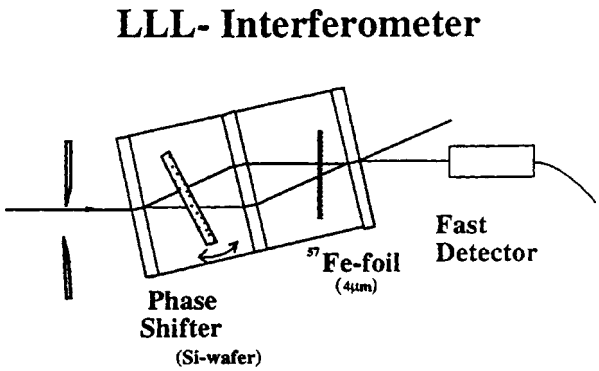

Figure 4. Schematic view of the experimental setup. In the triple-Laue interferometer a Si wafer is inserted as the phase shifter in front of an ^{57}Fe foil of the nuclear resonant scatterer. The interference oscillations were observed due to a phase shift introduced before nuclear resonant scattering which occurs with a certain time delay [21].

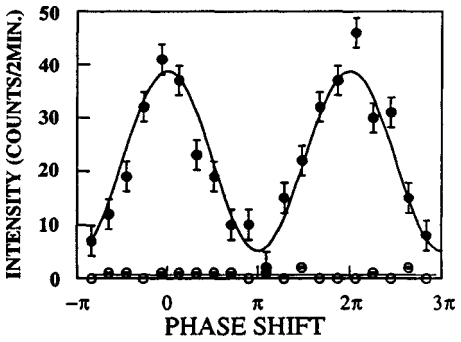

Figure 5. Interference oscillations with least squares fits for the energy at (•) and off (○) resonance. A high visibility interference oscillation is observed at resonance, while only the background fluctuation is observed off resonance [21].

Si wafer. A highly enriched (95.5%) ^{57}Fe foil of about 4 μm thickness was used as nuclear resonant scatterer. The fast detector was set for the interfering O-beam.

The time window for the measurements was set from 37 to 47 ns. Thus, only pulses resonantly scattered with time delay were counted in the following interference experiments, the transmitted prompt radiation being removed. Oscillations due to interference were measured by changing the relative phase between the two paths with the phase shifter. As a reference, the yield with the same time window was collected for the beams off resonance by tuning the monochromator by 156 meV away from the resonance energy. The collected data with least squares fits are shown in figure 5. A clear sinusoidal oscillation on a low background is seen for counts at resonance, whereas only the background fluctuations are seen for counts off resonance. The contrast was as high as the instrumental performance of the interferometer. In addition to the coherence of the two beams, the present experimental results show that the phase information before absorption in the nuclear resonance is transferred to the re-emitted

radiation field after the nuclear excitation. Since re-emission occurs with time delay, the phase transfer demands that the phase information is stored in the intermediate state for the time of this delay, say 40 ns.

It should be stressed here that typical Bose phenomena of the photon statistics in the X-ray regime can hardly be observed even with the use of SR of high brightness. Only the intensity correlation experiment was reported owing to the high brilliance of synchrotron radiation temporarily available in the Tristan main ring (KEK, Tsukuba, Japan) [22].

So the incident photon state for time-delayed interferometry can be considered as the single photon state. The phase information transfer is described through successive absorption and re-emission processes with some time delay by a single nucleus. Since the intermediate photon state between the absorption and the re-emission in the nuclear resonance can be considered as the vacuum state, particular attention is paid to the possibility of storing the phase information in the intermediate vacuum photon state which transfers the phase information to the re-emitted radiation field.

For simplicity, the interaction of the quantized field with two-level nuclei is considered here [23]. We denote the pulsed incident radiation field together with the nuclei by $|\Psi_i\rangle$. If one photon is present in mode $\mathbf{k}_0$ and the nuclei are in the ground state, this combined state, $|1_{\mathbf{k}_0}; \{g_i\}\rangle$, can be written in the form of a direct product:

$$|\Psi_i\rangle = \big|1_{\mathbf{k}_0}; \{g_i\}\big\rangle = \mathrm{e}^{\mathrm{i}\Phi} \cdot |1_{\mathbf{k}_0}\rangle \otimes \big|\{g_i\}\big\rangle, \tag{3.1}$$

where Φ represents the intrinsic phase of the radiation field. A similar notation is used for the combined system of an atom plus radiation field in the cavity experiments [20].

The intermediate state $|\Psi_m\rangle$ between the absorption and the re-emission of the photon is given by

$$\begin{aligned} |\Psi_m\rangle &= \mathrm{i} \sum_{\mathbf{K}} \hbar g'_{\mathbf{K}} \boldsymbol{\pi}^\dagger \cdot a_{\mathbf{K}} |\Psi_i\rangle \\ &= \mathrm{i} \sum_{\mathbf{K}} \hbar g'_{\mathbf{K}} \boldsymbol{\pi}^\dagger \cdot a_{\mathbf{K}} \big(\mathrm{e}^{\mathrm{i}\Phi} \cdot |1_{\mathbf{k}_0}\rangle \otimes \big|\{g_i\}\big\rangle\big) \\ &= \mathrm{i}\hbar g'_{\mathbf{k}_0} \mathrm{e}^{\mathrm{i}\Phi} |0_{\mathbf{k}_0}\rangle \otimes \big|\{g_{i(\neq j)}\}, \mathrm{e}_j\big\rangle. \end{aligned} \tag{3.2}$$

Here $g'_{\mathbf{K}}$ is the coupling constant of the magnetic-dipole interaction. The operator $\boldsymbol{\pi}^\dagger$ describes the transition of the nucleus from the ground state to the excited state and $\boldsymbol{\pi}$ denotes the reverse process. The operators $a^\dagger_{\mathbf{K}}$ and $a_{\mathbf{K}}$ describe, respectively, creation and annihilation of a photon in the mode $\mathbf{K}$. This clearly shows that, while the nucleus is excited, the phase information before absorption is stored in the combined system of nucleus plus radiation field.

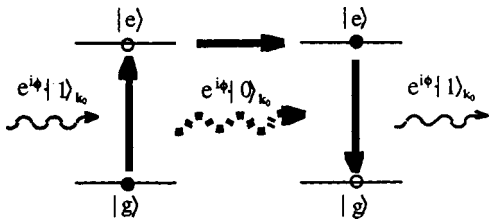

Figure 6. A model of phase information transfer in time-delayed nuclear resonant scattering. An incident single photon is absorbed and excites the nucleus. After some time interval the excited nucleus re-emits a photon. The phase information is stored in the vacuum photon state during the interval [21].

With some time delay after the primary absorption re-emission occurs. The final state $|\Psi_f\rangle$ is then given by

$$\begin{aligned}|\Psi_f\rangle &= -\mathrm{i}\sum_{\mathbf{K}} \hbar g'_{\mathbf{K}} \boldsymbol{\pi}\cdot a^{\dagger}_{\mathbf{K}}|\Psi_m\rangle \\ &= -\mathrm{i}\sum_{\mathbf{K}} \hbar g'_{\mathbf{K}} \boldsymbol{\pi}\cdot a^{\dagger}_{\mathbf{K}}\big(\mathrm{i}\hbar g'_{\mathbf{k}_0}\mathrm{e}^{\mathrm{i}\Phi}|0_{\mathbf{k}_0}\rangle \otimes \big|\{g_{i(\neq j)}\},\mathrm{e}_j\big\rangle\big) \\ &= \big(\hbar g'_{\mathbf{k}_0}\big)^2\mathrm{e}^{\mathrm{i}\Phi}|1_{\mathbf{k}_0}\rangle \otimes \big|\{g_j\}\big\rangle. \end{aligned} \tag{3.3}$$

This shows that the intrinsic phase factor $\mathrm{e}^{\mathrm{i}\Phi}$ is transferred to the final state through some time interval in the nuclear resonance, as was to be expected.

With eqs. (3.2) and (3.3) the phase information of the incident radiation field is shown to be transferred to the re-emitted beam in delayed nuclear resonant scattering. One may argue that the phase information is stored in the system of radiation field *plus* nucleus in the intermediate state. This combined system is described as the direct product of the two subsystems, and it is natural that the initial phase information to be transferred belongs to the state of the radiation field. In addition, the annihilation operator $a_{\mathbf{K}}$, which describes the absorption of the incident photon, operates directly on the state of the field. The intermediate state of the radiation field can be considered as the vacuum state including the phase information to be transferred. Figure 6 shows how in this scheme the intrinsic phase is transferred through the vacuum photon state in the nuclear resonance. It is important to note that in this scheme the vacuum state defined by the absence of any photons can take over its phase.

4. Interferometry of nuclear resonant scattering with large optical path difference

A beam obtained by nuclear resonant scattering is expected to have an extremely large longitudinal coherence of the order of more than a meter due to its extremely narrow energetic band width. X-ray interferometry is well suited for the observation of such an extremely large longitudinal coherence. It was, however, difficult to fabricate an interferometer which allowed the introduction of an optical path difference in the

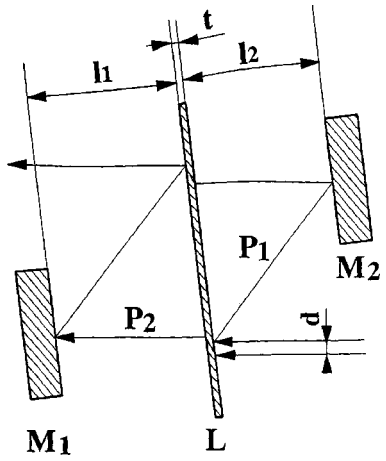

Figure 7. Design of the wave-front division BBB-interferometer with a long optical path difference [26].

X-ray regime. Only one experimental realisation was reported to demonstrate X-ray interferometry with an optical path difference [24]. This interferometer is a kind of Michelson interferometer which is well-known for the visible region [25]. This type of interferometer, however, is not suitable to introduce a large optical path difference, say more than 1 mm. Here an experimental realisation is shown of an X-ray interferometer of the wave-front division type with a large optical path difference, i.e., 4.2 mm [26]. The interference oscillations were observed using nuclear Bragg scattered X-rays from $^{57}Fe_2O_3$ as the incident beam.

The design of the interferometer is crucial; one candidate is the amplitude division interferometer, which has been commonly used as LLL-interferometer, and another is the wave-front division interferometer. The former seems to be easier to fabricate at first sight. Different sets of diffracting netplanes, however, are needed to introduce an optical path difference. This causes several difficulties, e.g., the choice of netplanes for fixed wavelength and/or the mechanical fabrication of the interferometer with exact dimensions. Although the latter requires a certain degree of transverse coherence of the incident beam, the use of one set of diffracting netplanes is feasible for its construction, which makes it much easier to estimate the performance.

The final design of the wave-front division interferometer with a large optical path difference was of the triple-Bragg (BBB) type and is shown in figure 7. A crystal plate L works as a beam splitter and analyzer. The plates M1 and M2 are mirrors. Asymmetric Si(8 8 0) Bragg reflections were used with an asymmetry parameter $b = 0.69$ at the resonant energy of ^{57}Fe ($\lambda = 0.86$ Å). The distances M1–L and M2–L were $l_1 = 21.65$ mm and $l_2 = 23.35$ mm, respectively, and the thickness of L was 1.1 mm. The optical path difference Δ is given by

$$\Delta = (l_2 - l_1)\left(\frac{1}{\sin(\Theta_B - \alpha)} + \frac{1}{\sin(\Theta_B + \alpha)}\right), \tag{4.1}$$

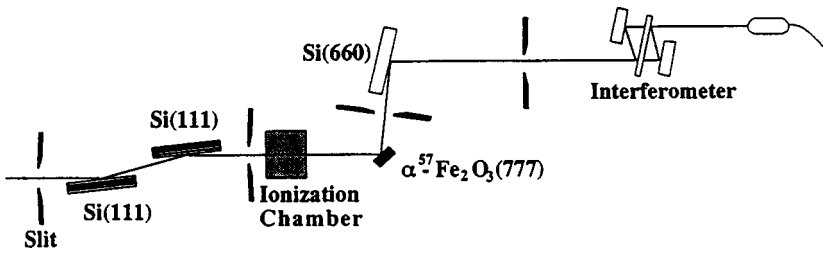

Figure 8. Schematic view of the interference experiments. The incident beam is monochramatized by a Si(1 1 1) monochromator and a $^{57}Fe_2O_3$ nuclear monochromator. In addition, it is collimated by an asymmetric Si(6 6 0) reflection and traverses the wave-front division BBB-interferometer [26].

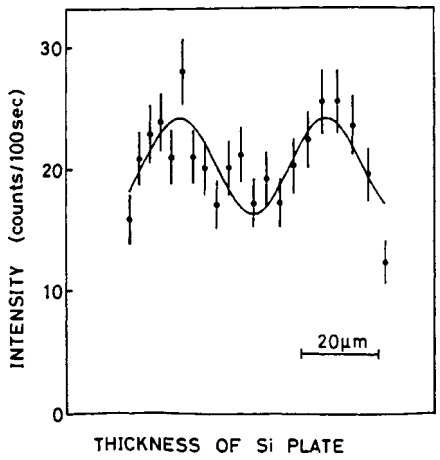

Figure 9. Interference oscillations of nuclear resonant scattering with a large path difference with least squares fits of the data [26].

where Θ_B and α represent the Bragg angle and the angle between the diffracting netplane and the crystal surface, respectively. Substituting $\Theta_B = 63.6^\circ$ and $\alpha = 20^\circ$, Δ is estimated to be 4.2 mm.

A schematic view of the experimental setup is shown in figure 8. The incident beam was monochromatized by a Si(1 1 1) double-crystal monochromator and successively reflected by the (7 7 7) reflection of a $^{57}Fe_2O_3$ single crystal which was placed in a magnetic field. This allowed nuclear resonant scattering only for the nuclear transitions with $\Delta m = \pm 1$. The Si collimator with asymmetric (6 6 0) reflection magnified the vertical beam cross-section 47 times from about 0.2 mm. In the BBB-interferometer the wave-fronts are displaced transversally by 2 mm at the exit.

The necessary transverse coherence of the incident beam was obtained with this collimator placed upstream of the interferometer. The beam cross-section was reduced to 5 mm(V) $\times$ 2 mm(H). The typical intensity of the beam after the interferometer was 0.2 cps in a NaI scintillation detector. As a phase shifter a silicon wafer of 370 μm thickness was inserted.

The throughput intensity of the beam from the interferometer is shown in figure 9 as a function of the phase difference between the two beams in the interferometer with least squares fits. The visibility, which is defined as the ratio between the amplitude of the oscillation to the mean intensity, was calculated to be about 20%. Taking the non-overlapping part of the beam into account the effective visibility was estimated to be one-third. In addition to the unequal beam intensity due to absorption in the phase shifter the finite source size and/or imperfection of each optical component in the experiments should be considered for further quantitative arguments on the loss of visibility for large optical difference interferometry.

5. Quantum beats from a vibrating resonant scatterer

In the field of nuclear resonant scattering quantum beat oscillations in the subsequent decay channel is one of the most interesting phenomena [14]. It reflects the coherence of the excited energy levels of nuclei split by hyperfine interaction. In addition, some important parameters in solid state physics, e.g., the isomer shift or the quadrupole splitting, can be obtained from the time spectra in time-domain Mössbauer spectroscopy. This beating in time results from slightly different level energies at the resonance. When one vibrates a resonant scatterer mechanically, magnetically or by ultrasound, the resonant energy can be shifted by the Doppler effect. When the vibrating resonant scatterer is inserted into one of the split beams in an X-ray interferometer, this enables us to observe a quantum beat oscillation due to the filtration of two beams with different energies.

A schematic view of the experimental setup is shown in figure 10. The delayed coincidence system as well as the monochromators were essentially the same as those for earlier work [16,21]. Stainless steel foils highly enriched to 91% in ^{57}Fe of about 2.5 μm thickness were used as nuclear resonant scatterers. They are inserted between the first and the second plate of the interferometer as a nuclear resonant filter. One of them was vibrated mechanically parallel to the beam by a linear motor. This induced a Doppler shift of the resonant energy at the scatterer. The vibrator was set at a constant

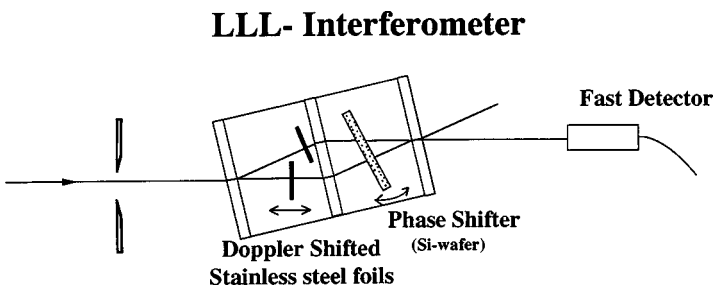

Figure 10. Schematic view of the experimental setup. In the triple-Laue interferometer a Si wafer is inserted as a phase shifter before the nuclear resonant scatterer consisting of stainless steel foils. The observed interference is due to the phase shift before the nuclear resonance with a certain time delay.

velocity for a Doppler shift ΔE $(=\hbar\Delta\omega) = \pm 2.17 \cdot 10^{-7}$ eV for forward and backward movements. A phase shifter of a parallel sided Si wafer was inserted between the second and the third plate of a symmetric triple-Laue interferometer. This induced a phase shift between the beams filtered out with different energy by the resonant scatterer. The phase shift ϕ given by this phase shifter was set at 0, $\pi/2$, π, and $3\pi/2$. A fast detector was set for the interfering O-beam.

According to the theoretical predictions the time spectrum of the quantum beat oscillation from the vibrating resonant scatterer is given by

$$\begin{aligned} \mathrm{I} &= \left| \frac{1}{\sqrt{2}} G(t) \mathrm{e}^{\mathrm{i}\omega_0 t} + \frac{1}{\sqrt{2}} G(t) \mathrm{e}^{\mathrm{i}\phi} \cdot \mathrm{e}^{\mathrm{i}(\omega_0 + \Delta\omega)t} \right|^2 \\ &= \frac{1}{2} \left| G(t) \right|^2 \left| 1 + \mathrm{e}^{\mathrm{i}(\phi + \Delta\omega t)} \right|^2 \\ &= \left| G(t) \right|^2 \cos(\phi + \Delta\omega t), \end{aligned} \tag{5.1}$$

where $G(t)$ and ω_0 represent, respectively, the envelope of the time evolution of the nuclear resonant forward scattering at the stainless steel foil and the frequency of the resonant scatterer at rest. The time evolution of $G(t)$ is expected to show a simple decrease in the case of the thin stainless steel foils used in the experiments. Thus an additional beating in the time spectrum is due to the quantum beat from the two different energies given by the mechanical vibration of the resonant scatterer. The time spectra of the throughput beam of the interferometer obtained for the backward movement of the resonant scatterer are shown in figure 11. Quantum beat oscillations

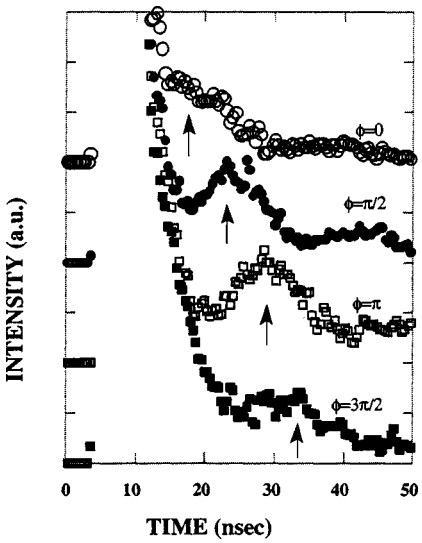

Figure 11. Time spectra of quantum beat oscillations due to a vibrating resonant scatterer. The phase shift ϕ induced by the phase shifter was set to 0, $\pi/2$, π, and $3\pi/2$. The period of the oscillations was determined by the Doppler-shifted energy at the vibrating resonant scatterer. Peaks of the oscillations are shifted according to the phase shift ϕ.

are clearly seen. The period of the oscillations is in good agreement with the given energy difference. For larger phase shifts ϕ the peaks of the oscillations shift to later time (see arrows in figure 11). When plotting the case for the forward movement of the resonant scatterer the peaks shift to earlier time, which is completely described by eq. (5.1).

Whether the incident beam can be described as an incoherent mixture or a wave packet, equivalent to a coherent superposition of plane waves, is under hot discussions [27]. The above experimental results show that beams with different energies in the interferometer are coherent after filtration by the resonant scatterer. It should be emphasized here that this requires coherence of the component with different energy of the filtered incident beam. In other words, the incident beam should be described as the coherent superposition of waves with different energy.

6. Dispersion at nuclear resonant scattering

The phase factor $e^{i\delta}$ due to the real part of an anomalous scattering factor f' is not accessible in an intensity measurement, where only the square of the amplitude can be observed. An X-ray interferometer using one split beam as a reference has been used as a powerful strategy for the precise measurements of f'. Here the interferometry is demonstrated between beams affected by nuclear resonant forward scattering by two ^{57}Fe enriched stainless steel foils with different thicknesses [28]. The time evolution of the nuclear resonant scattering reveals remarkable amplitude modulations of the wave field in the following decay. The X-ray dispersion at resonance with a certain thickness of the sample changes the sign of the amplitude in a certain time window. (Normally, there are a positive amplitude and a phase. Here, however, we refer to a positive and a negative amplitude, which are conventionally described with phases of 0 and π.) In and out of phase oscillations with respect to the transmitted prompt yield are shown for two time windows due to this difference in the sign of the *amplitude*.

A theoretical treatment of the time evolution of the nuclear resonant forward scattering was given for the case of pulsed SR [29]. For the case of n-fold foils, the time evolution of the amplitude as a function of delay time t is given by

$$G^A(t;n) = e^{in\varphi_0}\left\{\delta(t) - e^{(-i\omega_0 t-\tau/2)}\frac{n\xi_0}{\tau_0}\frac{J_1(2\sqrt{n\xi_0\tau})}{\sqrt{n\xi_0\tau}}\Theta(t)\right\}, \tag{6.1}$$

where

$$\Theta(t) = \begin{cases} 1, & t > 0, \\ 0, & t < 0, \end{cases} \qquad \tau = \frac{t}{\tau_0}, \tag{6.2}$$

τ_0 is the lifetime of the excited nuclear state, and φ_0 the phase shift due to scattering by electrons. The parameter ξ_0 is estimated to be 4.1876 for the stainless steel foils used in the experiments. The expected time evolution of the amplitude for the cases of $n = 1$ and 4, which are employed in the experiments, is shown in figure 12(a).

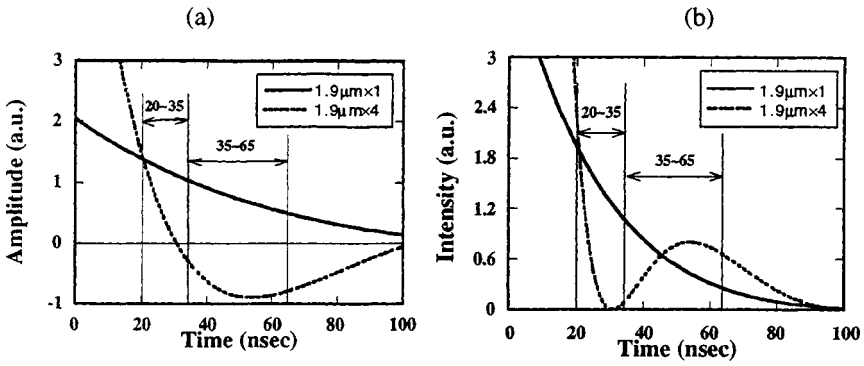

Figure 12. Expected time evolutions (a) of the amplitude and (b) of the intensity through nuclear resonant forward scattering. Stainless steel foils are 1- and 4-times 1.9 μm thick [28].

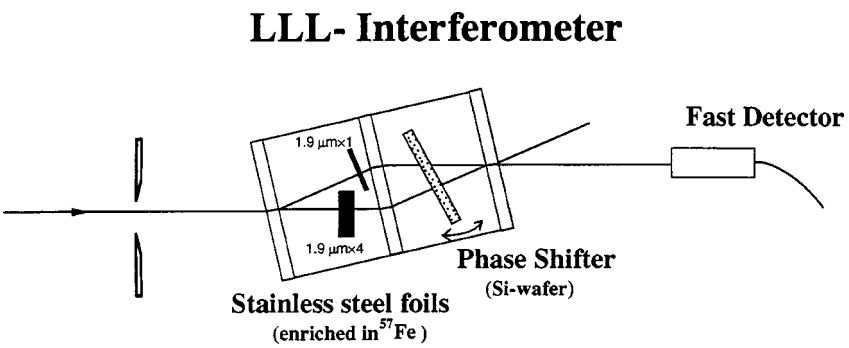

Figure 13. Schematic view of the interference experiments. The incident beam is monochromatized through successive monochromators and impinges on the interferometer. In the triple-Laue interferometer, the phase shifter, made of a Si wafer, and 1- to 4-fold 1.9 μm thick stainless steel foils are inserted [28].

The time evolution for $t > 0$ of the intensity is obtained as the absolute square of the amplitude in eq. (6.1):

$$I(t;n) = \left|G^A(t;n)\right|^2 \quad (t>0) \tag{6.3}$$

$$\propto n \cdot \mathrm{e}^{-\tau}\frac{\xi_0}{\tau}\left\{\mathrm{J}_1\left(2\sqrt{n\cdot\xi_0\cdot\tau}\,\right)\right\}^2. \tag{6.4}$$

The expected time evolution of the intensity is shown in figure 12(b). It is worth noting here that the amplitude between 31 and 103 ns for 4-fold foils is negative. In a conventional intensity measurement, however, there is no information about the sign of the *amplitude* shown in figure 12(a).

Let us consider the beam propagation in the interferometer, where 1- and 4-fold stainless steel foils are inserted into each beam path (figure 13). Here the oscillations collected for three different time gates are shown. The intensity $I_{t_1\sim t_2}$, collected with the time gate between t_1 and t_2, is given with the phase shift by an auxiliary phase

shifter ϕ by

$$I_{t_1\sim t_2} \propto \int_{t_1}^{t_2} \left|G^A(t;\,1) + \mathrm{e}^{\mathrm{i}\phi} G^A(t;4)\right|^2 \mathrm{d}t$$
$$= \frac{1}{2}\left\{1 + C_{t_1\sim t_2}\cos(\phi + 3\varphi_0)\right\}, \tag{6.5}$$

where $C_{t_1\sim t_2}$ represents the contrast of the interference pattern. Under the experimental conditions, while both Bessel functions $\mathrm{J}_1(2\sqrt{\xi_0\tau})$ and $\mathrm{J}_1(2\sqrt{4\,\xi_0\tau})$ are positive almost everywhere between 20 and 35 ns, one Bessel function $\mathrm{J}_1(2\sqrt{\xi_0\tau})$ is positive and the other $\mathrm{J}_1(2\sqrt{4\,\xi_0\tau})$ negative between 35 and 65 ns. This results in an equal phase shift to the prompt component of the sinusoidal oscillation for the time gate between 20 and 35 ns. In contrast, the intensity collected with the time gate between 35 and 65 ns oscillates out of phase – phase shift of π in addition to the common phase shift $3\varphi_0$ – to the prompt component.

The delayed coincidence system as well as the monochromators were the same as those for earlier work [16,21]. A Si single crystal LLL-interferometer was adjusted to give (2 2 0) reflections (figure 13). The cross-section of the incident beam was reduced to 5.0×0.2 mm^2 before the interferometer. Stainless steel foils enriched to 91% in ^{57}Fe were inserted between the first and the second plate of the interferometer as nuclear resonant forward scatterers. One of them was a 1-fold foil of about 1.9 μm thickness and the other was 4-fold. Each was inserted into each split beam path in the interferometer. As a phase shifter a 290 μm thick Si wafer was inserted between the second and the third plate of the interferometer. A relative phase was introduced by rotating this Si wafer. A fast detector was set for the interfering O-beam. The count rate without any gates represented the prompt signal. The yields influenced by the nuclear resonance were collected with two different time gates. They were adjusted to pick up the same $(+/+)$ and different $(+/-)$ signs of the amplitude in the time evolution of the nuclear resonant forward scattering through 1- and 4-fold foils. As shown in figure 12, one time gate (for the former case) was set between 20.1 and 34.6 ns, and the other (for the latter case) between 35.3 and 64.9 ns. For convenience we refer to these time gates as 20 and 35 ns, and 35 and 65 ns.

The observed interference patterns as a function of the relative phase are shown in figure 14. Clear sinusoidal oscillations for the prompt and for the two different delayed time gates were observed, the contrasts being 0.77(12), 0.56(7), and 0.53(8) for the prompt yield, the delayed yield between 20 and 35 ns, and the yield between 35 and 65 ns, respectively. Slight reductions of contrast are mainly caused by the incomplete superposition of the delayed amplitude shown in figure 12(a). It should be stressed here that the delayed yield between 20 and 35 ns oscillates in phase with the prompt yield, but that the delayed yield between 35 and 65 ns is out of phase with the prompt yield, the phase shift being π. This is well justified by the fact that, as for the Bessel function in eq. (6.1), the sign of the *amplitude* for the 4-fold foil with a delay between 35 and 65 ns is negative when propagating through the nuclear resonators, i.e., the ^{57}Fe enriched stainless steel foils.

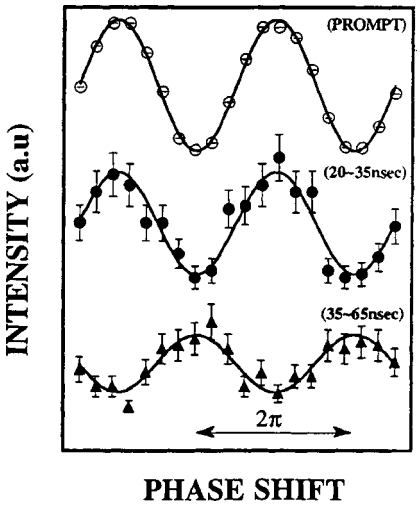

Figure 14. Interference oscillations with least squares fits. The yield gated between 20 ns and 35 ns oscillates in phase to the prompt signal. On the other hand, the yield gated between 35 ns and 65 ns oscillates out of phase (phase shift of π) [28].

In an application of the nuclear resonant scattering by SR to Mössbauer spectroscopy only the intensity as the absolute square of the amplitude, e.g., figure 12(b), is examined, by which the phase factor $e^{i\delta}$ vanishes. It is, however, possible with an interferometer to determine this factor, i.e., 0 and π in the present case. The present interferometry has confirmed more details of the time evolution of the nuclear forward scattering, which as a fitting function is strongly connected with the parameters of interest in time-domain Mössbauer spectroscopy.

The observed amplitude modulation is caused by the dispersion at the nuclear resonance, which causes a distinct phase velocity in a small range of the spectrum. In addition, the dispersion of the time-delayed scattering at an isolated nucleus is identified with a complex physical parameter. Its real part shows an anomalous dispersion and causes the corresponding phase velocity, and the imaginary part requires a narrow effective range of ω at the resonance. It is worth noting here that there is no amplitude modulation in the time evolution of the nuclear resonant forward scattering without distinct phase velocities due to the real part of the dispersion. The present performance of the X-ray interferometer yields observable consequences due to the real part of the dispersion, as in the precise measurements of f'.

7. Summary

Time-delayed interferometry with nuclear resonant scatterers highly utilizes the properties of SR. For instance, a pulsed collimated beam from the SR source permits the use of the perfect crystal interferometer with discrimination of the nonresonantly transmitted prompt component, which is unrealizable with a conventional radioisotope

source. Various characteristic interference effects can be observed on a macroscopic scale with the interferometer. The coherence of nuclear resonant scattering guaranteed the observations of

(i) interference between the beams emitted by different nuclei,

(ii) collective absorption and re-emission from a single photon state,

(iii) absorption of photons need not be accompanied by reduction, and

(iv) interferometry between (more than two) free-induction delayed signals.

Next, combined systems showed (i) phase information transfer through the vacuum photon state, and (ii) spontaneous emission with reasonable phase relation. This phase information transfer could be used as phase memory, which is not a digital but an analog memory. Moreover, optically significant experiments as well as further investigations of the time evolution of nuclear resonant scattering were performed. They are all impossible without the use of a "perfect crystal" interferometer, where the phase difference is the direct measure. It should be emphasized that Mössbauer nuclei were used as a cavity for X-rays in these experiments. Time-delayed interferometry can be used to observe temporal phenomena in nuclear resonant scattering; e.g., a perturbation applied between absorption and re-emission, an investigation of three combined subsystems, the observation of a quantized radiation field before and after nuclear resonant scattering in addition to the state of the nuclei would be of considerable interest. A quantitative measurement with a "perfect crystal" interferometer is expected to determine the degree of coherence in nuclear resonant scattering. Time-delayed interferometry has been established as a new and wide field of X-ray optics, which can be of help for fundamental, nuclear, and solid state physics.

References

[1] U. Bonse and M. Hart, Appl. Phys. Lett. 6 (1965) 155.
[2] U. Bonse and M. Hart, Z. Phys. 188 (1965) 154.
[3] U. Bonse and M. Hart, Z. Phys. 194 (1966) 1.
[4] A. Zeilinger, C.G. Shull, M.A. Horne and G.L. Squires, in: *Neutron Interferometry*, eds. U. Bonse and H. Rauch (Oxford Univ. Press, London, 1979) p. 48.
[5] A. Zeilinger, C.G. Shull, J. Arther and M.A. Horne, Phys. Rev. A 28 (1983) 487.
[6] P. Becker, K. Dorenwendt, G. Ebeling, R. Lauer, W. Lucas, R. Probst, H.-J. Rademacher, G. Reim, P. Seyfried and H. Siegert, Phys. Rev. Lett. 46 (1981) 1540.
[7] U. Bonse and G. Materlik, Acta Crystallogr. A 31 (1975) 232.
[8] M. Hart and D.P. Siddons, Proc. Roy. Soc. London A 376 (1981) 465.
[9] Y. Hasegawa and S. Kikuta, Z. Phys. B 93 (1994) 133.
[10] Y. Hasegawa and S. Kikuta, Phys. Lett. A 195 (1994) 43.
[11] G. Materlik, C.J. Sparks and K. Fischer, *Resonant Anomalous X-Ray Scattering. Theory and Applications* (Elsevier, New York, 1994).
[12] L. Allen and J.H. Eberly, in: *Optical Resonance and Two-level Atoms*, Interscience Monographs and Texts in Physics and Astronomy, Vol. 28 (Wiley/Interscience, New York, 1975).

[13] T.C. Farrar and E.D. Becker, *Pulse and Fourier Transform NMR. Introduction to Theory and Methods* (Academic Press, New York, 1971).
[14] J.B. Hastings, D.P. Siddons, U. van Bürck, R. Hollatz and U. Bergmann, Phys. Rev. Lett. 66 (1991) 770.
[15] T. Hellmuth, A.G. Zajonc and H. Walther, in: *New Technique and Ideas in Quantum Measurement Theory* (The New York Academy of Sciences, 1986) p. 108.
[16] Y. Hasegawa, Y. Yoda, K, Izumi, T. Ishikawa, S. Kikuta, X.W. Zhang, H. Sugiyama and M. Ando, Japan J. Appl. Phys. 33 (1994) 772.
[17] D. Bohm, in: *Quantum Mechanics* (Prentice-Hall, Englewood Cliffs, NJ, 1951).
[18] J.D. Franson, Phys. Rev. Lett. 62 (1989) 2205.
[19] M. Horne, A. Shimony and A. Zeilinger, Phys. Rev. Lett. 62 (1989) 2209.
[20] A.P. Kasantsev, G.I. Surdutovich and V.P. Yakovlev, *Mechanical Action of Light on Atoms* (World Scientific, Singapore, 1990).
[21] Y. Hasegawa, Y. Yoda, K. Izumi, T. Ishikawa, S. Kikuta, X.W. Zhang and M. Ando, Phys. Rev. Lett. 75 (1995) 2216.
[22] Y. Kunimune, Y. Yoda, K. Izumi, M. Yabashi, X.W. Zhang, T. Harami, M. Ando and S. Kikuta, J. Synchrotron Rad. 4 (1997) 199.
[23] R. Loudon, in: *The Quantum Theory of Light*, 2nd ed. (Clarendon Press, Oxford, 1983) p. 162.
[24] A. Appel and U. Bonse, Phys. Rev. Lett. 67 (1991) 1673.
[25] A.A. Michelson, Amer. J. Sci. 122 (1881) 120.
[26] K. Izumi, T. Mitsui, M. Seto, Y. Yoda, T. Ishikawa, X.W. Zhang, M. Ando and S. Kikuta, Japan J. Appl. Phys. 34 (1995) 5862.
[27] V.L. Lepore, Phys. Rev. A 48 (1993) 111.
[28] Y. Hasegawa, Y. Yoda, K. Izumi, T. Ishikawa, S. Kikuta, X.W. Zhang and M. Ando, Phys. Rev. B 50 (1994) 17748.
[29] Yu. Kagan, A.M. Afanas'ev and V.G. Kohn, J. Phys. 12 (1979) 615.